Application of the rotating ring disc electrode technique to water oxidation by surface-bound molecular catalysts.

Authors: Javier J. Concepcion,[1] Robert A. Binstead,[1] Leila Alibabaei,[1] Thomas J. Meyer[1*]

Affiliations:

[1]University of North Carolina at Chapel Hill, Department of Chemistry.

*Correspondence to: tjmeyer@unc.edu

Synthesis and characterization of catalysts. The syntheses of **1** and **2** follow a similar procedure which is shown in Figure S1.

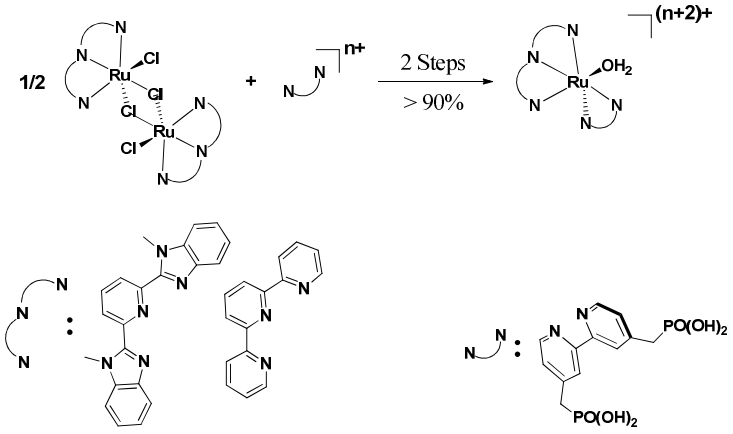

Figure S1. Synthetic strategy for the preparation of **1** and **2**.

It involves reaction of the dichloro-bridged dimers $[Ru(tpy)Cl]_2Cl_2$ and $[Ru(Mebimpy)Cl]_2Cl_2$ with 4,4'-$(PO(OH)_2CH_2)_2$-bpy to give the corresponding chloro complexes $[Ru(NNN)(4,4'-(PO(OH)_2CH_2)_2\text{-bpy})(Cl)]^+$. This step is followed by abstraction of the chloro ligand with neat triflic acid, in-situ reduction of oxidized species with aqueous ascorbic acid and precipitation of the corresponding triflate salts with a large excess of lithium triflate. Analytically pure samples are obtained this way. ^{1}H-NMR, UV-Vis and electrochemistry match with previously reported syntheses.[1,2]

Catalyst loading on planar electrodes. ITO slides (3.5×1 cm) were sonicated in isopropanol for 20 min. The isopropanol was decanted off and the procedure repeated one more time followed by the same procedure twice with water. The slides were air-dried prior to immersion in a ~ 10^{-4} M solution of the catalysts in 0.1 M HNO_3. Full surface loadings of ~ 1×10^{-10} mol/cm^2 (determined electrochemically by integrating the area under a CV wave) were obtained in less than 30 min.

Preparation of *nano*-ITO or *nano*-ATO modified ring-disc electrodes. ITO or ATO nanoparticles (Sigma-Aldrich, <50 nm) were suspended in 9:1 MeOH:H_2O (~ 7 mg/mL). The suspension was sonicated for 20 min to disperse the nanoparticles and shaken by hand before use. The already assembled ring-disc electrode (glassy carbon disc and platinum ring, Pine Instruments) was held upside down on a ring stand. 12 μL of the nanoparticles suspension was carefully added to the glassy carbon disc with a micropipette. The Teflon that separates the disc from the ring prevents the suspension from flowing to the platinum ring. The solvent mixture was allowed to evaporate and the modified electrode was allowed to dry for at least 20 min. The catalysts were loaded by immersing the modified ring-disc electrode in ~ 10^{-4}-10^{-3} M solutions of the catalysts in 0.1 M HNO_3. Surface loadings were determined electrochemically by integrating the area under a CV wave. The projected surface area occupied by the catalyst was determined by the surface area of the glassy carbon disc (0.196 cm^2).

Rotating ring-disc electrode (RRDE) experiments. RRDE experiments were performed with a Pine Instruments bipotentiostat and rotator. The working electrode was the previously described *nano*-ITO or *nano*-ATO modified ring-disc electrode (*nano*-ITO-RRDE). The reference electrode was a standard Ag/AgCl electrode (PINE model RREF0021) mounted in a Vycor tipped glass tube with fresh electrolyte to avoid chloride contamination of the primary electrolyte. The counter electrode was a platinum wire coil in an isolated glass tube with fine glass frit separator (PINE model AFCTR5). All the experiments were performed with 0.1 M $HClO_4$.

For linear sweep voltammetry at a rotating disc electrode (RDE) the current at the disc is given by the Koutecký-Levich equation, eq 1.[3] The first term, i_K, is the kinetic current, *i.e.*, the current in the absence of mass transport effects. The second term is the diffusional current. It depends on the rotation rate (ω), the area of the electrode (A), the diffusion coefficient of the substrate (D_0), the kinematic viscosity of the liquid (ν) and the substrate concentration (C_0).

$$\frac{1}{i} = \frac{1}{i_K} + \frac{1}{0.62nFAD_0^{2/3}\omega^{1/2}\nu^{-1/6}C_0^*} \qquad \text{eq 1}$$

At high rotation rates the diffusional term tends to zero. The substrate concentration at the electrode surface is the same as in the bulk and the current at the disc is determined by the kinetics at the electrode. For water oxidation in aqueous solutions, water is the substrate and the limiting current in RDE experiments is independent of the rotation rate and the scan rate. This was confirmed by performing RRDE experiments at scan rates of 5, 10 and 20 mV/s. The currents were the same as long as the catalyst loading was the same. Thus, the catalytic current for water oxidation in these experiments is dictated by the turnover frequency of the catalyst at the applied voltage E ($k_{cat}(E)$), the surface loading of the catalyst (Γ), and the area of the electrode (A), eq 2.[4]

$$i_{cat} = nFA\Gamma k_{cat}(E) \quad \text{eq 2}$$

Determination of the product(s) from O_2 reduction at Pt. For quantification purposes, it is important to know the products from O_2 reduction at platinum (H_2O *vs* H_2O_2) and their ratio. Reduction to H_2O is a 4-electron process and the only correction needed for the ring current associated for this process is the collection efficiency since water oxidation to O_2 is also a 4-electron process. Reduction to H_2O_2 is a 2-electron process and the ring current associated for this process has to be corrected for collection efficiency and for the factor of 2 ratio between the 4-electron oxidation at the disc and the 2-electron reduction at the ring. To this end, RRDE experiments were conducted in oxygen-saturated 0.1 M $HClO_4$ solution with a Pt-disc Pt-ring assembly. The potential of the disc was scanned from 1.0 V to -0.05 V vs NHE at 10 mV/s while the potential of the ring was held constant at 1.13 V vs NHE. H_2O_2 generated at the disc from O_2 reduction will be oxidized to O_2 at the ring under these conditions, Figure S8. The blue trace shows the cathodic current at the disc due to reduction of O_2. The red trace shows the current at the ring. The lack of anodic current indicates that no H_2O_2 is generated and O_2 is completely reduced to water under these conditions. When the experiment was repeated with a degassed solution, no anodic current was observed, Figure S9.

Water oxidation RRDE experiments. 0.1 M $HClO_4$ solutions were degassed by bubbling nitrogen for 20 min. The disc potential was scanned from 1.0 V to 1.79 V *vs* NHE while the ring potential was held constant at -0.017 V *vs* NHE to detect O_2 or at 1.13 V *vs* NHE to detect H_2O_2 (oxidation of H_2O_2 to O_2 is diffusion-limited at this potential at pH 1).

Collection efficiency. Osmium(II) tris-(4,4'-dimethyl-2,2'-bipyridine) perchlorate, $[Os(dmb)_3](ClO_4)_2$, was used to determine the collection efficiency of our glassy carbon-disc Pt-ring RRDE assembly. We chose this complex over iron ferricyanide because of its higher electron transfer self-exchange rate and better reversibility of its $Os^{III/II}$ couple, Figure S6. RRDE experiments at various rotation rates were performed in degassed pH 7 phosphate buffer solutions 1.0 mM in $[Os(dmb)_3](ClO_4)_2$. The disc potential was scanned from 0.3 V to 1.05 V *vs* NHE at 10 mV/s while the ring potential was held constant at 0.25 V *vs* NHE to reduce Os^{III} generated at the disc during the oxidative scan. Figure S7A shows a plot of ring current *vs* disc current at different rotation rates. The current at the ring is 24.9 % of the disc current for all rotation rates, as shown by the linear fit with $R^2 = 0.9994$. Figure S7B shows the actual data for the RRDE experiments with the ring currents corrected for the 24.9 % collection efficiency.

Scanning Electron Microscopy (SEM). SEM analysis was performed on FEI Helios 600 Nanolab Dual Beam System. The sample was stuck on a double sided sticky carbon tape and mounted on an aluminum sample holder. An accelerating voltage of 5kV with a beam current of 0.69 nA was used. All images were acquired at a working distance close to 4mm.

Instrumentation. The ring-disc electrode assembly comprised PINE models AFE6M electrode shaft, AFE6R1PT ring assembly, and ACE6DC050GC hands-off glassy carbon disc assembly.

The bipotentiostat was a PINE model AFCBP1 with AKCBP6251 PCI interface kit and AfterMath software. The rotator was a PINE model AFMSRCE. The cell was a 125 ml glass vessel fitted with B14/20 side joints, B24/25 center joint with an AC01TPA6M gas purged center bearing assembly.

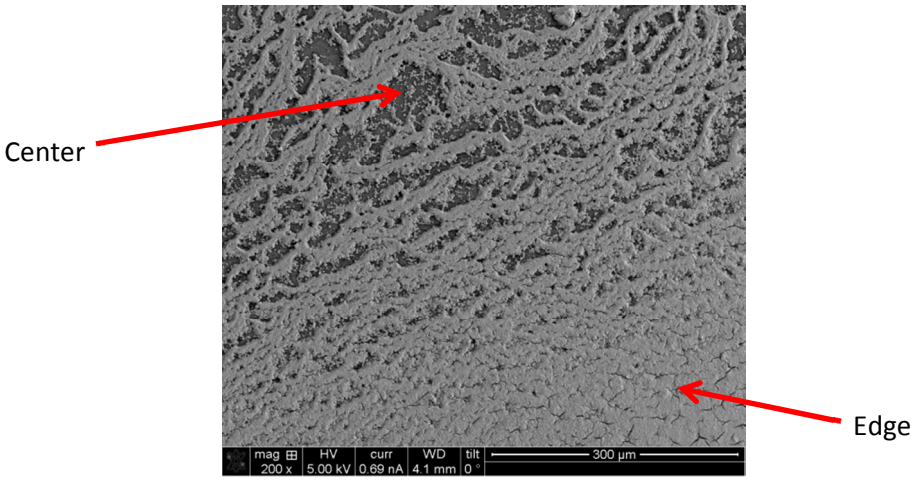

Figure S2. SEM images of the nano-ITO-modified glassy carbon disc at 200x magnification.

Scheme S1. Water oxidation cycle for *nano*-2.

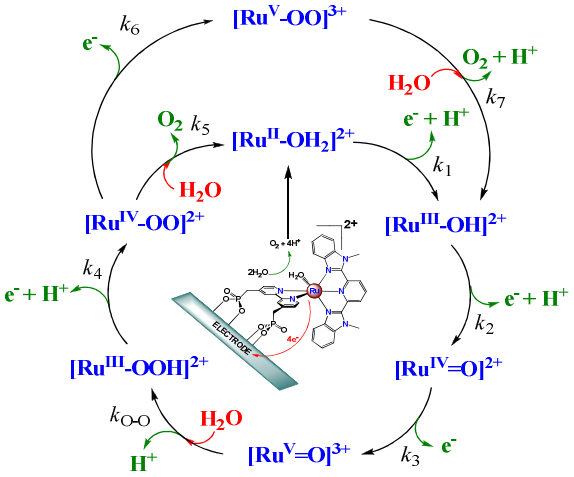

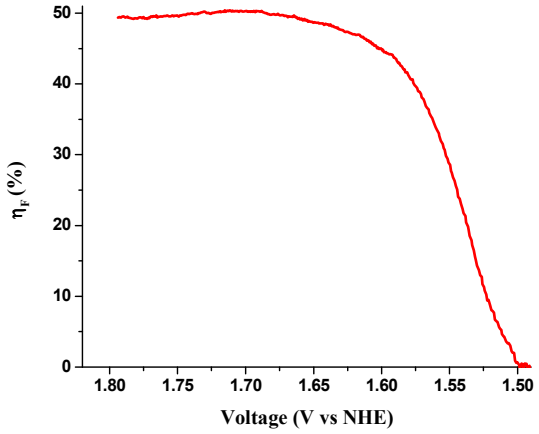

Figure S3. Faradaic efficiency η_F for electrocatalytic oxygen generation (calculated from the data in Figure 3 with background and collection efficiency corrections) as a function of applied potential for *nano*-**2** in 0.1 M $HClO_4$.

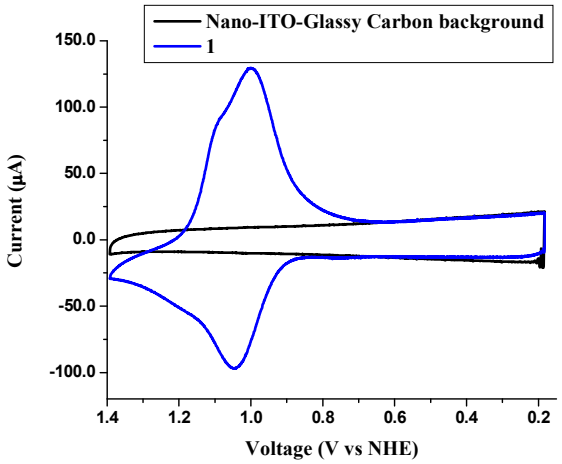

Figure S4. Blue: CV of **1** on a *nano*-ITO-Glassy carbon in 0.1 M $HClO_4$. Scan rate: 100 mV/s. Black: Background of the *nano*-ITO-Glassy carbon electrode under the same conditions.

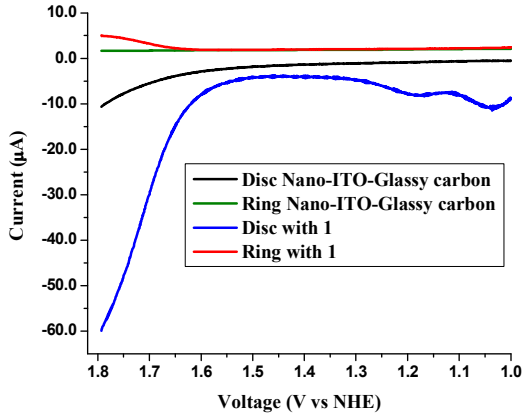

Figure S5. Rotating ring disc voltammogram in 0.1 M $HClO_4$. The potential of the disc was scanned from 1.00 V to 1.79 V at 10 mV/s. The rotation rate was 500 rpm. The potential of the ring (platinum) was held constant at -0.017 V. Black: Nano-ITO-modified glassy carbon disc current. Green: corresponding ring current. Blue: current with **1** attached to *nano*-ITO-modified glassy carbon disc. Red: corresponding ring current with **1** present on modified disc electrode.

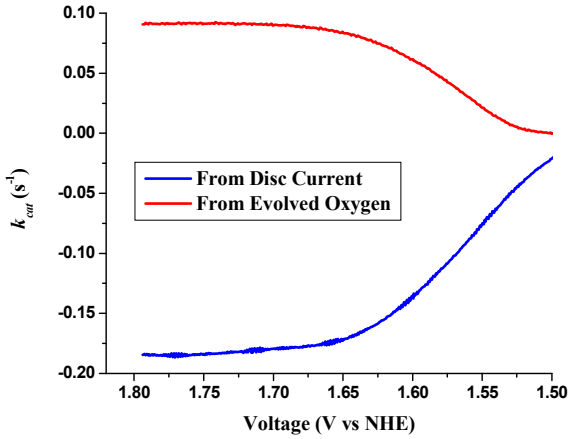

Figure S6. Turnover frequencies (as $k_{cat}(E)$), eq 2, calculated from the data in Figure 3 with background and collection efficiency corrections, as a function of applied potential for *nano*-**2** in 0.1 M $HClO_4$. The data have been corrected for background current in the absence of **2**. It has also been corrected (×4.0) for the collection efficiency (24.9 %) of the ring electrode, see text.

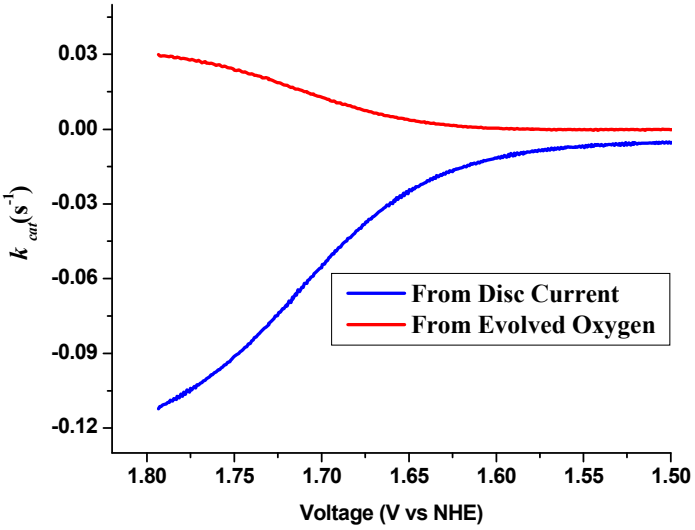

Figure S7. Turnover frequencies (as $k_{cat}(E)$), eq 2, calculated from the data in Figure S5 with background and collection efficiency corrections) as a function of applied potential for *nano*-**1** in 0.1 M $HClO_4$. The data have been corrected for background current in the absence of **1**. It has also been corrected (×4.0) for the collection efficiency (24.9 %) of the ring electrode.

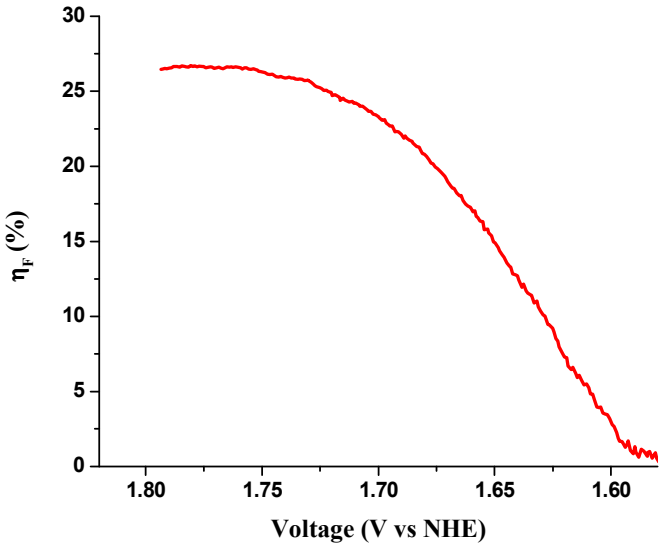

Figure S8. Faradaic efficiency η_F for electrocatalytic oxygen generation (calculated from the data in Figure S5 with background and collection efficiency corrections) as a function of applied potential for *nano*-**1** in 0.1 M $HClO_4$.

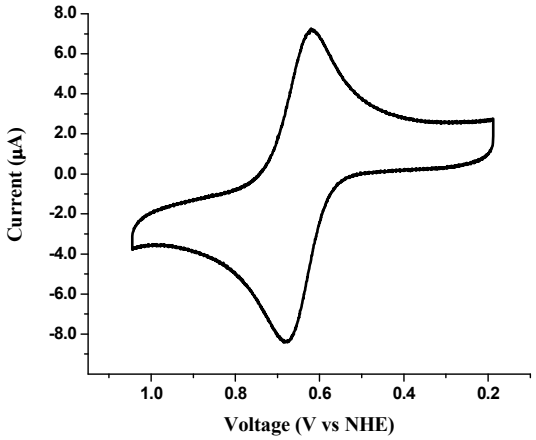

Figure S9. Cyclic voltammogram for *tris*-(4,4'-dimethyl-2,2'-bipyridine)osmium(II) perchlorate ($[Os(dmb)_3](ClO_4)_2$) in 0.1 M phosphate buffer (pH = 7.0).

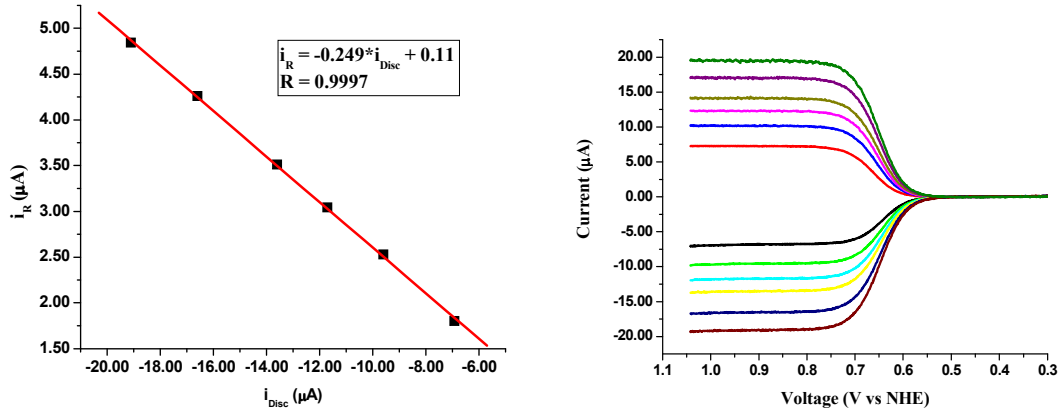

(A) **(B)**

Figure S10. **(A)** Plot of ring vs disc currents from LSV experiments at 250, 500, 750, 1000, 1500 and 2000 rpm for the oxidation (disc) and reduction (ring) of 1 mM $Os(dmb)_3^{2+}$ in 0.1 M phosphate buffer at pH = 7.0. The linear fit shows the collection efficiency of 24.9%, independent of rotation rate. **(B)** Raw data from the previous experiment with the ring current corrected for background and collection efficiency.

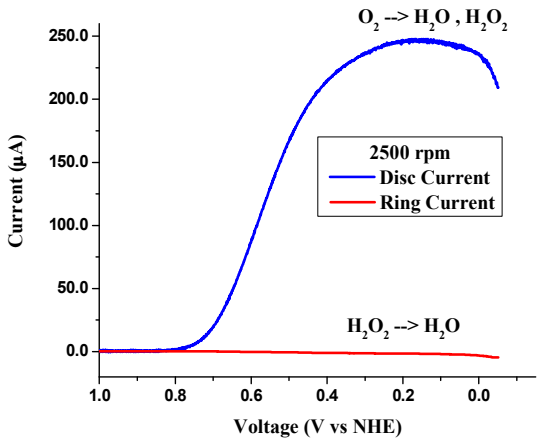

Figure S11. Rotating ring disc voltammogram in oxygen-saturated 0.1 M $HClO_4$. The potential of the platinum disc was scanned from 1.00 V to -0.05 V at 10 mV/s. The rotation rate was 2500 rpm. The potential of the ring (platinum) was held constant at 1.13 V to oxidize any generated H_2O_2 at the disc to O_2. The blue trace shows the cathodic current at the disc due to reduction of O_2. The red trace shows the current at the ring. The lack of anodic current indicates that no H_2O_2 is generated and O_2 is completely reduced to water under these conditions.

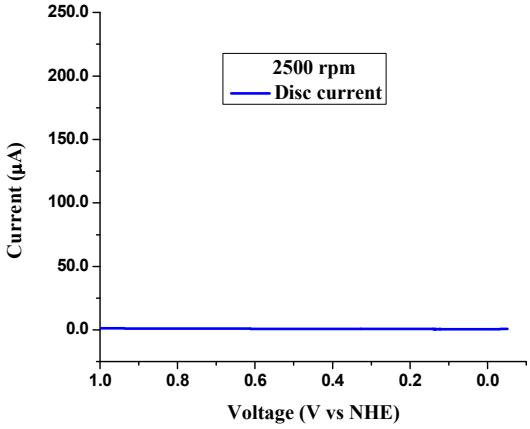

Figure S12. Linear sweep voltammogram in degassed 0.1 M $HClO_4$. The potential of the platinum disc was scanned from 1.00 V to -0.05 V at 10 mV/s. The rotation rate was 2500 rpm. Notice scale is the same as Figure S11.

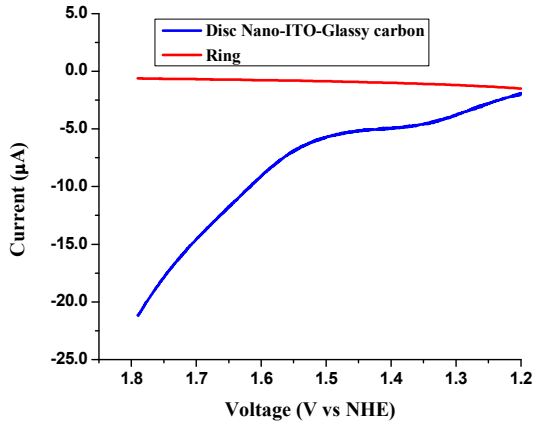

Figure S13. Rotating ring disc voltammogram in 0.1 M $HClO_4$. The potential of the disc was scanned from 1.00 V to 1.79 V at 10 mV/s. The rotation rate was 500 rpm. The potential of the ring (platinum) was held constant at +1.13 V. Blue: current with **1** attached to *nano*-ITO-modified glassy carbon disc. Red: corresponding ring current with **1** present on modified disc electrode. The lack of oxidative current due to oxidation of hydrogen peroxide to oxygen indicates that no H_2O_2 is being generated at the disc.

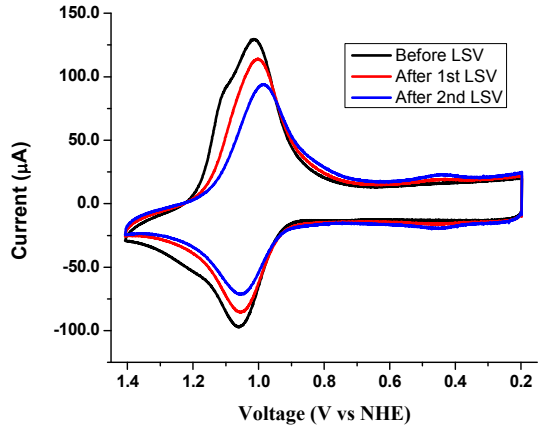

Figure S14. CVs of **1** on a *nano*-ITO-Glassy carbon in 0.1 M $HClO_4$. Scan rate: 100 mV/s. Black: Before LSV to 1.79 V as in Figure S5. Red and blue: after 1st and 2nd LSV scans to 1.79 V. Note decreased current for the Ru^{IV}=O/Ru^{III}-OH_2 wave after oxidative LSV scans due to generation of the anated species Ru^{III}-ClO_4. Anation is more efficient on planar ITO. It can be reversed by reducing the complex to Ru^{II}-ClO_4 which quickly generates Ru^{II}-OH_2. This behavior is not observed for **2** and will be discussed in a separate manuscript.

References.

(1) Concepcion, J. J.; Jurss, J. W.; Norris, M. R.; Chen, Z. F.; Templeton, J. L.; Meyer, T. J. *Inorg. Chem.* **2010**, *49*, 1277.
(2) Kiyota, J.; Yokoyama, J.; Yoshida, M.; Masaoka, S.; Sakai, K. *Chem. Lett.* **2010**, *39*, 1146.
(3) Bard, A. J. F., Larry R. *Electrochemical Methods: Fundamentals and Applications*; 2nd ed.; John Wiley & Sons, Inc., 2001.
(4) Elliott, S. J.; McElhaney, A. E.; Feng, C. J.; Enemark, J. H.; Armstrong, F. A. *J. Am. Chem. Soc.* **2002**, *124*, 11612.